Identification of non-essential regions in nucleocapsid protein of porcine reproductive and respiratory syndrome virus for replication in cell culture

Feifei Tan, Zuzhang Wei, Yanhua Li, Rong Zhang, Jinshan Zhuang, Zhi Sun, Shishan Yuan*

Department of Swine Infectious Diseases, Shanghai Veterinary Research Institute, Chinese Academy of Agricultural Sciences, No. 518 Ziyue Road, Shanghai 200241, China

ARTICLE INFO

ABSTRACT

Nucleocapsid (N) protein of porcine reproductive and respiratory syndrome virus (PRRSV) plays a central role in virus replication. In this study, serial N- and C-terminal truncations of N protein were performed in the context of type 2 PRRSV infectious cDNA clone, and our results revealed that a stretch of inter-genotypic variable N terminal residues aa 5–13 (^{5}NGKQQKKK^{13}K) and the last four inter-genotypic variable aa residues (^{120}SPS^{123}A) at the C terminus of N protein were dispensable for type 2 PRRSV infectivity. All the recovered deletion mutant viruses had spontaneous mutations in the N coding region, including substitution, deletion and insertion. We re-engineered the additional internal deletion with or without the original C-terminal deletion back into wild-type APRRS and found that the internal domain spanning the inter-genotypic variable residues 39–42 (^{39}KGP^{42}G) and conserved residues 48–52 (^{48}KNPE^{52}K), respectively, were dispensable for type 2 PRRSV viability. These results demonstrated that N protein contains non-essential regions for virus viability in cell culture. Such dispensable regions could be utilized as insertion site for foreign tag expression and the rescued viruses could be the candidates for marker vaccine.

© 2011 Elsevier B.V. All rights reserved.

1. Introduction

Porcine reproductive and respiratory syndrome virus (PRRSV) is a single-strand, positive-sense RNA virus, and is a member of the family *Arteriviridae*, together with equine arteritis virus (EAV), lactate dehydrogenase-elevating virus (LDV), and simian hemorrhagic fever virus (SHFV). *Arteriviridae* and *Coronaviridae* are classified as members of the order *Nidovirales*, mainly based on their similar replication and transcription strategy (den Boon et al., 1991; Gorbalenya et al., 2006; Snijder and Meulenberg, 1998). Two genotypes of PRRSV have been classified, (European) type 1 and (North American) type 2, Lelystad virus (LV) (Wensvoort et al., 1992) and VR2332 (Benfield et al., 1992) are the representative strains of two types, respectively. PRRSV virion consists of at least seven structural proteins, including glycoprotein 2 (GP2) (Meulenberg and Petersen-den Besten, 1996), GP3 (de Lima et al., 2009), GP4 (van Nieuwstadt et al., 1996), GP5, and unglycosylated envelope (E) protein (Wu et al., 2005), membrane (M) protein, and nucleocapsid (N) protein (Bautista et al., 1996). Structural proteins of arteriviruses are expressed via a nested set of subgenomic mRNAs (sgmRNAs) formed by a unique discontinuous transcription process (de Vries et al., 1990; Meng et al., 1996; Nelsen et al., 1999). The common 5′ leader sequence of sgmRNAs is derived from the 5′ proximal untranslated region (UTR). The leader-body junction sequence can be amplified by sgmRNA-specific RT-PCR (Chen et al., 1993; den Boon et al., 1996; Meulenberg et al., 1993; Nelsen et al., 1999; Zheng et al., 2010).

N protein is the most abundant component of the virion and plays a crucial role in virus assembly. Generally, type 1 and type 2 PRRSV N proteins consist of 128 and 123 amino acids (aa), respectively. However, Stadejek et al. (2008) reported that N protein of type 1 exhibits size polymorphism, the number of amino acid residues varies from 124 to 130. Although N protein is one of the inter-genotypically conserved proteins, LV and VR2332 share only 64% identity at the amino acid level (Dea et al., 2000). N protein is assembled into an icosahedral nucleocapsid in the form of disulfide-linked homodimer (Wootton and Yoo, 2003), and the C-terminal half of PRRSV N protein is believed to be the dimerization domain (Spilman et al., 2009). The N-terminal half of N protein is enriched in basic amino acids and intrinsically disordered, which are common properties of RNA-binding proteins (Daginakatte and Kapil, 2001; Doan and Dokland, 2003; Yoo et al., 2003).

The crystal structure of the C-terminal dimerization domain comprises two antiparallel β-sheet floors superposed by two long α helices and flanked by two N- and C-terminal α helices (Doan and Dokland, 2003), as shown in Fig. 1A. The structure is homologous to that of EAV (Deshpande et al., 2007), and surprisingly, has a fold similar to that of severe acute respiratory syndrome-associated coronavirus (Yu et al., 2006). By replacing each amino
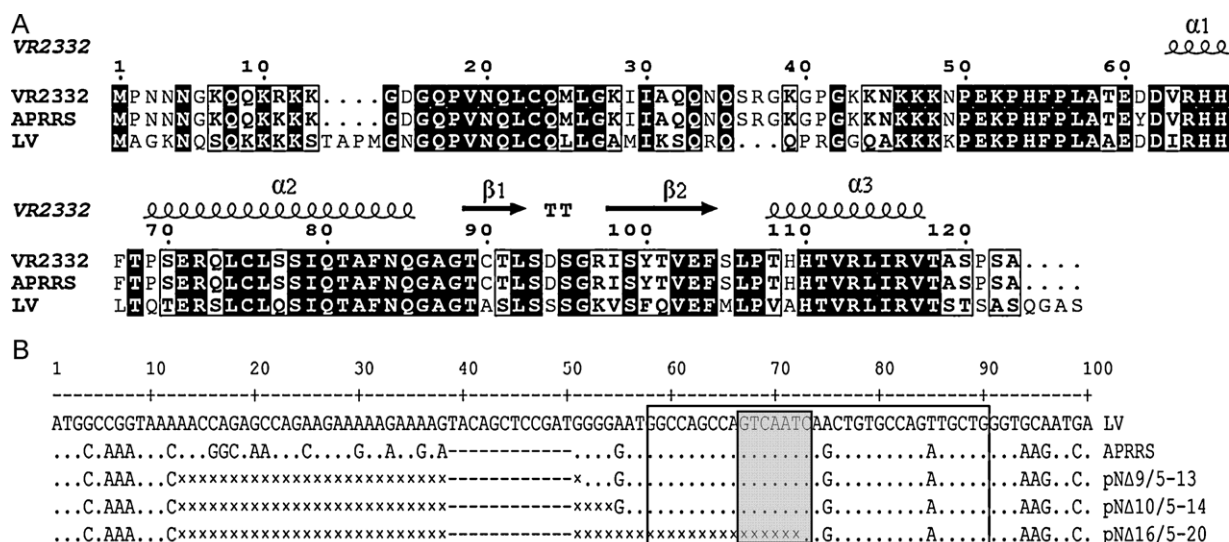
Fig. 1. (A) Multiple sequence alignment of PRRSV N proteins. Highly conserved residues are shaded in black, whereas partially conserved residues are indicated by open boxes. The secondary structure of the C-terminal domain of VR2332 N protein is indicated at the top (Doan and Dokland, 2003) (PDB ID: 1P65). Alignment of the N sequence from type 2 strain VR2332 (GenBank ID: AY150564), the wild-type APRRS (GenBank ID: GQ330474) in this study and type 1 strain LV (GenBank ID: M96262). (B) Sequence alignment of the first 100 nt sequence of ORF7 of LV, APRRS and N-terminal deletion mutants, the identical sequence with LV is denoted as dot while natural sequence deletion compared with LV designated as dash line. The engineered deletion is represented by asterisk. The 34 nt that was documented to be essential for RNA replication of LV (Verheije et al., 2002) is indicated in the open box, the 7 nt sequence which had kissing interaction with 3′UTR is indicated by shaded box.

acid with proline, Wootton et al. (2001) demonstrated that the 111–117 aa substitution of type 2 PRRSV N protein reduces the conformational-dependent monoclonal antibody (McAb) binding significantly. Therefore, the C-terminus of N protein is important for maintaining the local and/or the overall configuration of the PRRSV N protein. Verheije et al. (2001) reported that C-terminal six amino acids of N protein are non-essential for virus infectivity of type 1 PRRSV. These authors also indicated that the N-terminal and internal regions of N protein cannot tolerate deletion.

As shown in Fig. 1A, N protein is intra-genotypically conserved and only one (D61) out of the 123 aa of type 2 prototypic strain, VR2332, is different from the APRRS strain (Y61) used in this study. Several inter-genotypically conserved domains were observed too. In addition, crystal structure of C-terminal dimerization domain except for the last 5 aa of VR2332 N protein was determined (Doan and Dokland, 2003). In this study, to further illustrate the roles of the terminal and internal aa residues of N protein in type 2 PRRSV replication, particularly in viral viability. We performed serial deletions at the N- and C-termininal of N protein in the context of full-length cDNA clone pAPRRS. We found that type 2 PRRSV contained extensive regions that were dispensable for virus viability in cell culture. These results are of great significance for foreign gene expression and genetic engineered vaccine development.

2. Materials and methods

2.1. Cells and plasmids

MARC-145 cells were grown in minimal essential medium (MEM) (Sigma) complemented with 10% fetal bovine serum (FBS) (Invitrogen), and maintained in MEM with 2% FBS at 37 °C with 5% CO_2.

Type 2 PRRSV infectious cDNA clone pAPRRS (Yuan and Wei, 2008) was used as the wild-type control in all experiments. Its complete genomic sequence was available as GenBank accession number GQ330474. pBSX was a shuttle plasmid that cloned the Spe I-Xho I region (nt 13117–15520) of APRRS genome into the pBluescript SK(+) vector (Fermentas). p7USC was constructed by inserting Asc I immediately after the stop codon of ORF7.

2.2. Site-directed mutagenesis of PRRSV N protein

N-terminal deletion was performed from the fifth amino acid to retain the integrity of ORF6. Fragments containing the corresponding deletion region were generated using the mutagenic PCR method as described before (Yu et al., 2009), pBSX was the template. Then the Spe I-Xho I fragment of pAPRRS was replaced by the analogous fragments derived from mutagenic PCR products. Internal deletion mutants were constructed in the same manner.

C-terminal deletion mutants were constructed based on the full-length clone p7USC. The fragments containing the desired deletion were amplified by PCR, Asc I was introduced in anti-sense primers (Table 1), and the sense primer was SpeF (Table 1). The Spe I-Asc I fragment of p7USC was replaced by the PCR fragments carrying the desired deletion.

For the construction of plasmids that contained primary engineered deletions and spontaneous mutations, appropriate fragments were prepared by RT-PCR products from the viral cell culture supernatants. The amplified fragments between Xba I and Xho I were swapped into the corresponding region of pAPRRS. All full-length clones of mutants were verified by Sma I mapping and nucleotide sequencing.

2.3. Transfection and rescue of mutant virus

Full-length plasmids were prepared with QIAprep Spin Miniprep kit (QIAGEN). MARC-145 cells were seeded in six-well plates and grown to 80% confluence. The monolayer cells were transfected with 1 μg plasmid using 3 μl FuGene HD regent (Roche) according to the manufacturer's instructions. After visible CPE was observed (about 72 h posttransfection for wild-type APRRS) and 80% of the monolayer cells were detached, the culture supernatants were collected and labeled as Passage (P) 0 viruses. The wild-type and recovered mutant viruses were passaged in MARC-145 cells five times to gain P1–P5 virus stocks. At least three further passages were performed if no visible CPE was observed after transfection.

Table 1
Primers used for PCR.

Name[a]	Sequence (5′–3′)[b]	Usage[c]
SF14991	CTTGTTAAATATGCCAAATAAC(△)AAGAAGGGGGATGGCCAGCCAG	△ 5–11
SR15049	CTGGCTGGCCATCCCCCTTCTT(△)GTTATTTGGCATATTTAACAAG	△ 5–11
SF15011M	CCTTGTTAAATATGCCAAATAAC(△)AAGGGGGATGGCCAGCCAGTCA	△ 5–12
SR15055M	TGACTGGCTGGCCATCCCCCTT(△)GTTATTTGGCATATTTAACAAGG	△ 5–12
SFND5-13	CCTTGTTAAATATGCCAAATAAC(△)GGGGATGGCCAGCCAGTCAATC	△ 5–13
SRND5-13	GATTGACTGGCTGGCCATCCCC(△)GTTATTTGGCATATTTAACAAGG	△ 5–13
SFND5-14	CCTTGTTAAATATGCCAAATAAC(△)GATGGCCAGCCAGTCAATCAGC	△ 5–14
SRND5-14	GCTGATTGACTGGCTGGCCATC(△)GTTATTTGGCATATTTAACAAGG	△ 5–14
SFND5-20	CCTTGTTAAATATGCCAAATAAC(△)CAGCTGTGCCAGATGCTGGGTAAG	△ 5–20
SRND5-20	CTTACCCAGCATCTGGCACAGCTG(△)GTTATTTGGCATATTTAACAAGG	△ 5–20
SF15105M	GCAAAACCAGTCCAGAGGT(△)AAGAAAAACAAGAAGAAAAACCCGG	△ 39–42
SR15148M	CCGGGTTTTTCTTCTTGTTTTTCTT(△)ACCTCTGGACTGGTTTTGC	△ 39–42
SF15116	GACCGGGAAAGAAAAACAAGAAG(△)CCCCATTTTCCTCTGGCGACTG	△ 48–52
SR15175	CAGTCGCCAGAGGAAAATGGGG(△)CTTCTTGTTTTTCTTTCCCGGTC	△ 48–52
ASR15348-6	AA<u>GGCGCGCC</u>TCA(△)GACGCGAATCAGGCGCAC	△ 118–123
ASR15351-5	AA<u>GGCGCGCC</u>TCA(△)TGTGACGCGAATCAGGCG	△ 119–123
ASR15351-4	AA<u>GGCGCGCC</u>TCA(△)TGCTGTGACGCGAATCAG	△ 120–123
ASR15357-3	AA<u>GGCGCGCC</u>TCA(△)TGATGCTGTGACGCGAAT	△ 121–123
SpeF	GAAGGCCACTTG<u>ACTAGT</u>GTTTACG	Sense primer for C-terminal mutants
SF14413	CTGATCGA CCTCAAAAGAGTTGTGCTTG	RT-PCR for N gene sequence
SR15497	CAAT TAAATCTTACCCCCACACGGTCG	RT-PCR for N gene sequence
Qst	GAGTGACGAG GA<u>CTCGAG</u>CGCATGCTTTTTTTTTTT TTT	Reverse transcription primer
SF12	GTGTTGGCTCTATGCCTTGAC	RT-PCR for sgmRNA7 detection
SR15284	CTCCACAGTGTAACTTATCCTCC	RT-PCR for sgmRNA7 detection
SRN3ASC	AA<u>GGCGCGCC</u>TCATGCTGAGGGTGATGCTG	Reverse primer for p7USC

[a] Prefixes: SF, forward PCR primer; SR, reverse PCR primer.
[b] Restriction sites introduced are underlined.
[c] △ indicates amino acids deletion.

2.4. Immunofluorescent assay

MARC-145 cells were transfected with plasmids of wild-type or mutants. Intracellular expressions of nsp2 and N were visualized by immunofluorescence staining at 48 hpt and 72 hpt, respectively, the protocol was same with that described before (Yu et al., 2009). The McAbs against nsp2 and N protein (MR40) (Wootton et al., 1998) were kindly donated by Dr. Ying Fang at South Dakota State University. Alexa Fluor 568 goat anti-mouse IgG (H + L) (Invitrogen) was used as a secondary antibody.

2.5. RT-PCR and nucleotide sequencing

Viral RNA was extracted from cell supernatants using QIAamp Viral RNA kit (QIAGEN), and treated with TURBO DNase (Ambion) to eliminate input genomic DNA according to the manufacturers' instructions. First-strand cDNA was synthesized using Reverse Transcriptase XL (AMV) (Takara) and anti-sense primer Qst (Table 1). The fragment containing the N gene was amplified by Taq DNA polymerase (Takara) using primer pairs SF14413 and SR15497. The PCR products were purified using TIANgel Mini Purification Kit (TIANGEN) and sequenced directly. The full-length genome of the recovered viruses was amplified by five primer pairs as described previously (Yuan and Wei, 2008), and the primer sequences were available upon request.

The leader-body junction sites of PRRSV were detected by sgmRNA-specific RT-PCR (Nelsen et al., 1999; Zheng et al., 2010). As shown in Fig. 3B, SF12 (nt 12–32) and SR15284 (nt 15284–15306) are the primer pairs of sgmRNA7 amplification of APRRS as described before (Yu et al., 2009).

2.6. Viral plaque purification

For the recovered P0 viruses that had a mixed population, plaque purification was performed. The transfected cell supernatants of C△3/121–123 and N△48–52 were used to infect MARC-145 cells at a MOI of approximately 0.01. After 1 h incubation, cell monolayer was overlaid with 2× MEM (Invitrogen) supplemented with 4% FBS and 2% low melting agarose (Promega). Well-isolated plaques were passaged onto fresh MARC-145 cells. RNA was extracted and RT-PCR was performed as previously described, then the N gene was sequenced.

2.7. Growth kinetics of the rescued viruses

MARC-145 cells were infected with wild-type and P5 rescued viruses at ∼0.01 MOI. Cell culture supernatants were collected at various times after infection. Titers were determined by standard $TCID_{50}$ assay. Three independent titrations were performed and the mean value was used for determination of the viral multi-step growth-curve.

3. Results

3.1. Generation of N- and C-terminal deletion mutants

Overlapping genes are a dominant feature of arterivirus genome, and there are 11 nucleotides that overlap between ORF6 and ORF7. Therefore, N-terminal deletion mutants were truncated from the fifth residue of ORF7 to ensure the integrity of ORF6. Inter-genotypic aa sequence alignment indicated that the LV strain (type 1) contains four extra aa residues (TAPM) than APRRS (type 2) immediately upstream of the inter-genotypically conserved region from [14]G of APRRS (Fig. 1A). It was therefore possible that this variable region plays little role in type 2 PRRSV N functionality. Accordingly, we constructed five deletion mutants that comprised residues 5–11, 12, 13, 14 and 20 at the N terminus, which were designated as pN△7/5–11, pN△8/5–12, pN△9/5–13, pN△10/5–14 and pN△16/5–20, respectively (Fig. 2A).

We also wanted to investigate the C-terminal requirements of N protein for type 2 PRRSV viability. To this end, a series of C-terminal truncation mutants were constructed. Firstly, a recombinant full-length clone p7USC containing an Asc I immediately after the stop codon of ORF7 was constructed (Fig. 2B, D). Transfection assay demonstrated that the Asc I insertion did not affect viral infectivity, and the rescued virus 7USC had similar growth
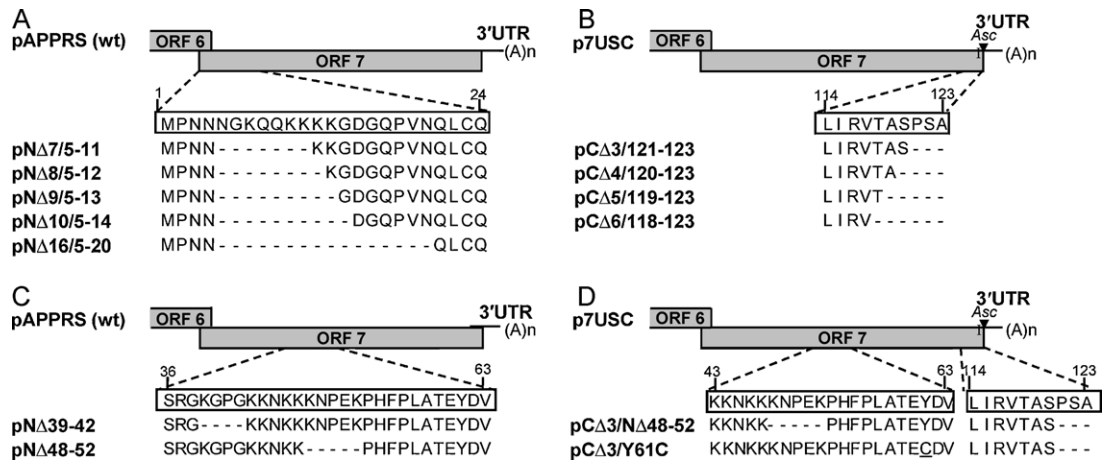
Fig. 2. Schematic diagram of PRRSV N protein deletion mutants. Gray box indicates part of the viral genome, and dashed line represents the deleted residues. pAPRRS was the wild-type full-length clone. p7USC was a full-length infectious cDNA clone that contained an *Asc* I site after the stop codon of ORF7. (A) Schematic drawing of N-terminal deletion mutants; (B) graphic representation of C-terminal deletion mutants; (C) construction strategy of internal deletion mutants; (D) schematic drawing of double mutants containing the primary C-terminal engineered deletion together with a second-site mutation. The "C" underlined in pCΔ3/Y61C indicates the mutated residue.

properties with the wild-type virus APRRS (Fig. 4B). Therefore, p7USC was used as the backbone for constructing C-terminal truncations, which contained residues 121–123, 120–123, 119–123, and 118–123 deletions, named as pCΔ3/121–123, pCΔ4/120–123, pCΔ5/119–123 and pCΔ6/118–123, respectively (Fig. 2B).

3.2. The N-terminal variable region was dispensable for PRRSV viability, while the inter-genotypically conserved region was vital for viral replication

To define whether the N-terminal deletions affect virus replication, full-length clones pNΔ7/5–11, pNΔ8/5–12, pNΔ9/5–13, pNΔ10/5–14, pNΔ16/5–20, and the wild-type pAPRRS, were transfected into MARC-145 cells. Intracellular expression of non-structural protein 2 (nsp2) and N protein was determined by immunofluorescence assay (IFA) at 2 and 3 days post-transfection (dpt), respectively, which indicated the genomic RNA replication and sgmRNA transcription properties of the mutants. As shown in Fig. 3A, all but pNΔ16/5–20 displayed nsp2 and N protein expression, but the fluorescence intensity was different. It was noteworthy that there were only several single cells stained for mutant pNΔ10/5–14, suggesting virus spreading between neighboring cells was affected. Moreover, no fluorescent signal was detected in the case of pNΔ16/5–20 (even after prolonged incubation at 7 dpt; data not shown), indicating that deletion of residues 5–20 ([5]NGKQQKKKKGDGQPV[20]N) might have blocked both virus replication and transcription. In the parallel transfection experiments, visible cytopathic effect (CPE) appeared for the wild-type pAPRRS as well as for mutants pNΔ7/5–11, pNΔ8/5–12 and pNΔ9/5–13. The longer deletion mutants pNΔ10/5–14 and pNΔ16/5–20, however, produced no infectious particles even after three further passages. These results demonstrated that the N-terminal residues 5–13 of N protein were non-essential for virus infectivity in cultured cells.

We next investigated the possible blockage for the N-terminal deletion mutants that failed to produce progeny viruses. Two sgm-RNAs (sgmRNA7.1 and sgmRNA7.2) of ORF7 have been defined in type 2 PRRSV infected cells (Nelsen et al., 1999; Zheng et al., 2010). As outlined in Fig. 3B, total RNAs of cells transfected with pNΔ9/5–13, pNΔ10/5–14, pNΔ16/5–20 and pAPRRS, respectively, were extracted and sgmRNA7-specific RT-PCR was performed as previously described (Yu et al., 2009; Zheng et al., 2010). As shown in Fig. 3C, the two expected bands representing sgm-RNA7.1 and sgmRNA7.2 were amplified from cells transfected with

wild-type pAPRRS, pNΔ9/5–13 and non-viable pNΔ10/5–14, but the band of pNΔ10/5–14 was weaker than others, indicating the lower transcription level than others. This was consistent with the IFA result and further demonstrated that sgmRNA transcription of pNΔ10/5–14 was down-regulated. However, pNΔ16/5–20 showed no sign of sgmRNA7 transcription (Fig. 3C) which was coincident with the IFA results against N protein expression (Fig. 3A).

3.3. Growth property and genetic stability of N-terminal deletion viruses

To assess their genetic stability, the rescued viruses NΔ7/5–11, NΔ8/5–12 and NΔ9/5–13 were serially passaged five times to establish virus stocks of P 1–5 virus. The supernatants of each passage were collected, and the cDNA fragment [nucleotides (nt) 14413–15497] containing ORF7 was amplified by RT-PCR. Nucleotide sequencing analysis confirmed that the engineered deletions were retained in all of the passaged viruses. However, several spontaneous mutations appeared when compared with wild-type virus APRRS. Another independent transfection experiment was carried out to confirm the occurrence of spontaneous mutations. The spontaneous mutations of the N-terminal deletion mutant viruses at P5 in two independent experiments were summarized in Fig. 5A. Almost all of the spontaneous mutations were different in two experiments. The spontaneous mutation nt T15355C (aa S120P) existed in NΔ9/5–13 was identical with that in mutant virus NΔ8/5–12 in experiment 1. Most of the spontaneous mutations emerged at P1 could be stably passaged to P5.

Given that N plays multiple functions in virus replication process, it was necessary to investigate whether additional genetic alterations were present in other genomic regions. In doing so, a total of five overlapping cDNA fragments were amplified by RT-PCR, followed by direct nucleotide sequencing. The consensus sequence of the full-length genome of mutant virus NΔ9/5–13 (P5) was assembled and showed no other detectable mutations besides the detected S120P mutation in N coding region. We also determined the sequence of 5'UTR, 3'UTR and M coding region of other mutant viruses, and found no additional genetic alterations.

To further quantitatively assess the growth behavior of the recovered N-terminal deletion mutant viruses in cultured cells, multiple-step growth curves were determined for P5 of rescued viruses NΔ7/5–11, NΔ8/5–12 and NΔ9/5–13. As depicted in Fig. 3D, virus NΔ7/5–11 and NΔ8/5–12 had similar growth kinetics with the parental APRRS. The mutant virus NΔ9/5–13 reached
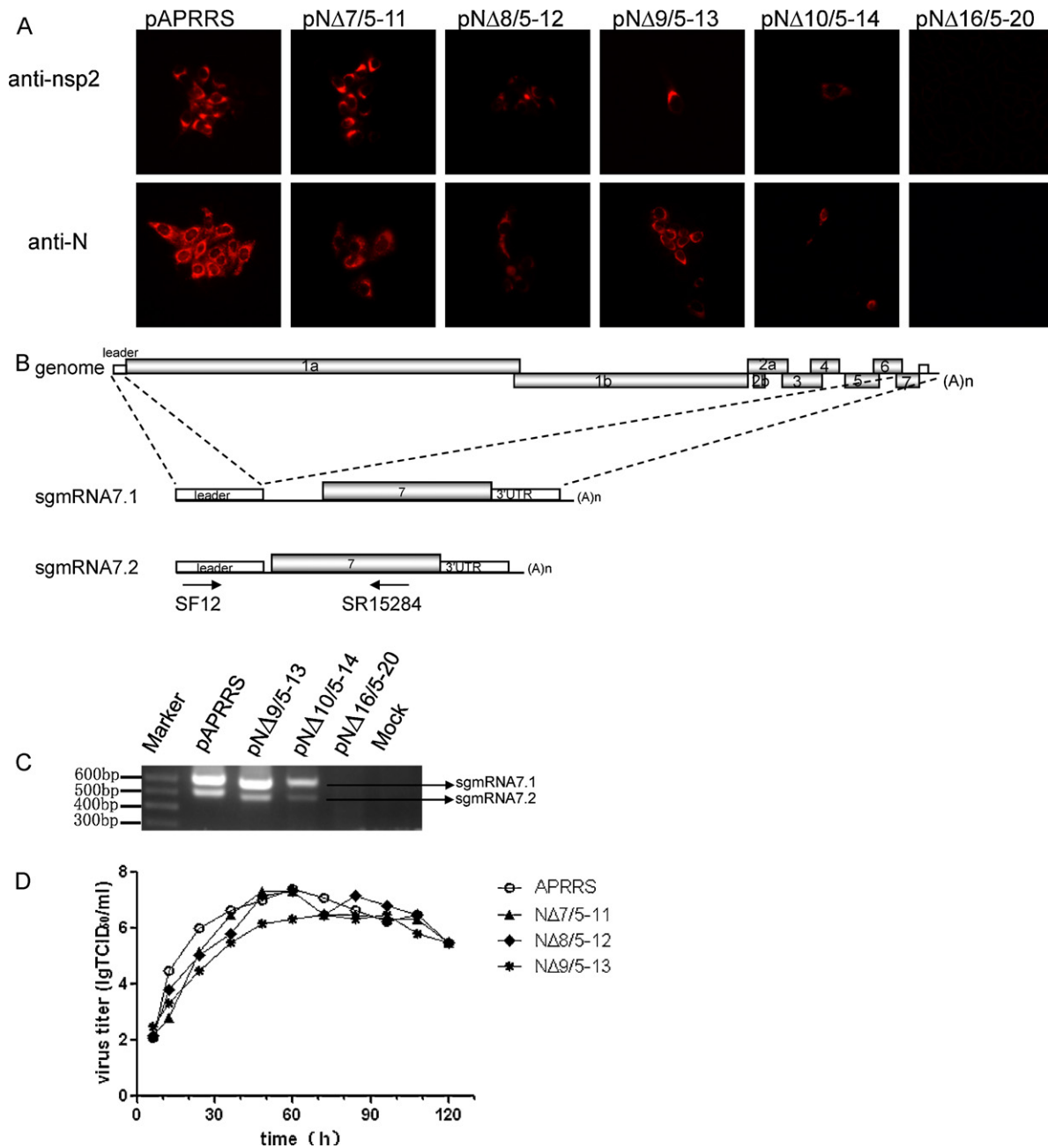
Fig. 3. Virological and genetic properties of N-terminal deletion mutants. (A) Intracellular nsp2 and N expression of mutants. MARC-145 cells were transfected with plasmids of pAPRRS, pNΔ7/5–11, pNΔ8/5–12, pNΔ9/5–13, pNΔ10/5–14 and pNΔ16/5–20 as indicated. Expression of nsp2 and N was visualized by immunofluorescence staining at 48 and 72 hpt, respectively. (B) Schematic drawing of PRRSV genome and sgmRNA7, sgmRNA 7.1 and sgmRNA7.2 represents the two sgmRNAs of type 2 PRRSV N protein. SF12 and SR15284 indicate the positions of RT-PCR primer pairs. (C) Identification of leader-body junction sequence of N-terminal deletion mutants by sgmRNA7-specific RT-PCR. The two bands in pAPRRS, pNΔ9/5–13, and pNΔ10/5–14 represent the identified sgmRNA 7.1 and sgmRNA 7.2. (D) Multiple growth curves on MARC-145 cells. Cells were infected with P5 wild-type APRRS, and recovered P5 N-terminal deletion mutant viruses at ∼0.01 MOI. Infectious virus released into the supernatants was collected and monitored at different times post-infection.

the peak titer at 72 h post-infection (hpi), which was 12 h delayed compared with APRRS, and the titer was nearly 100-fold lower than that of the wild type APRRS (Fig. 3D). This suggested that a larger deletion at the N-terminal of the N protein adversely affected virus replication process, and the spontaneous mutations in the rescued viruses may account for the growth difference.

3.4. The last four residues at the C terminus were non-essential for virus infectivity

We next attempted to define the role of the C-terminal unstructured residues for virus replication. Upon transfection of C-terminal deletion mutants, the intracellular expression of nsp2 and N protein were IFA positive for all mutants (Fig. 4A), though only a few positive cells were detected for pCΔ5/119–123 and pCΔ6/118–123, indicating the RNA synthesis level was reduced. Moreover, the MARC-145 cells transfected with mutants pCΔ3/121–123 and pCΔ4/120–123 developed typical PRRSV CPE, albeit it was delayed by 48 h compared with the parental p7USC. No CPE was observed for the larger deletion mutants pCΔ5/119–123 and pCΔ6/118–123, in spite of three additional passages. This was confirmed by RT-PCR with SF14413/SR15497 which showed no sign of infectious particles. These results indicated that the last 4 aa (^{120}SPS^{123}A) at the C terminus of type 2 PRRSV N protein were dispensable for virus
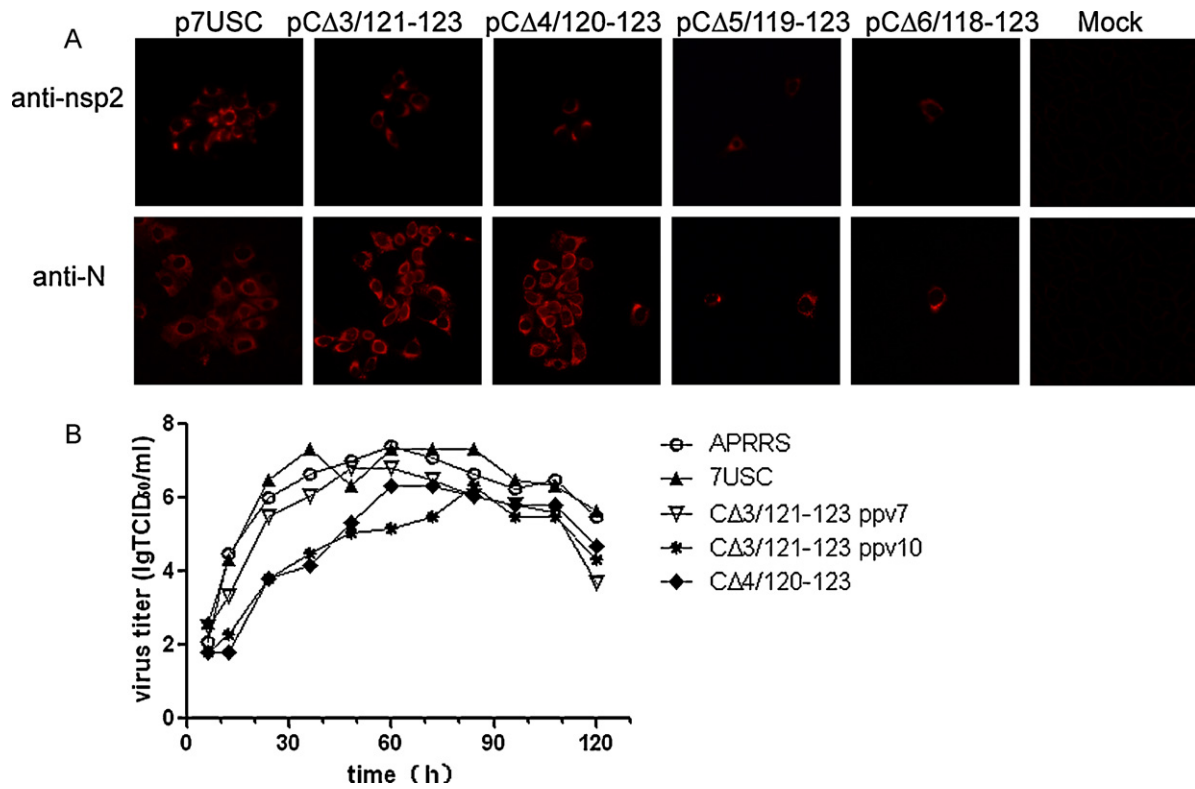
Fig. 4. Virological characteristics of C-terminal deletion mutants. (A) Intracellular nsp2 and N expression of C-terminal deletion mutants, pCΔ3/121–123, pCΔ4/120–123, pCΔ5/119–123 and pCΔ6/118–123, while p7USC and mock-transfected cells were used as controls. (B) Multiple growth curves of P5 7USC and C-terminal mutant viruses on MARC-145 cells.

viability, which was 2 aa upstream of the previous result based on LV strain (Verheije et al., 2001).

3.5. Genetic and virological properties of C-terminal viable mutants

The recovered C-terminal deletion viruses were also passaged for assessment of their genetic stability. The presence of the engineered deletions was confirmed by RT-PCR and nucleotide sequencing at all five passages for the recovered viruses CΔ3/121–123 and CΔ4/120–123. However, direct nucleotide sequencing of the RT-PCR products of CΔ3/121–123 displayed ambiguous sequence at some positions of ORF7, suggesting that the RT-PCR products contained a mixed population. We then performed plaque purification assay for transfectant virus CΔ3/121–123 (P0). A total of 20 plaques were picked and nucleotide sequencing of RT-PCR product (nt 14413–15497) displayed no ambiguity for an individual plaque. Collectively, we found three different types of spontaneous substitutions including nt T15178C, A15179G and A15319G, which resulted in aa Y61H, Y61C and T108A substitution, respectively (Fig. 5B). Surprisingly, two types of additional deletions (aa 39–42 and 48–52) were found (Fig. 5B). In an effort to assess the variety of the spontaneous mutations, we repeated the transfection experiment, plaque purification and RT-PCR, which showed only one type of additional mutation (nt A15179G (aa Y61C)) (Fig. 5B).

Mutant virus CΔ4/120–123 was analyzed in the same manner. The analysis revealed different spontaneous mutations in two independent transfections, including E51G substitution and a 3-aa insertion (Fig. 5B). The full-length genome sequence of CΔ4/120–123 (P5) containing the E51G mutation showed no further mutation in the other genomic regions. Surprisingly, the 9-nt sequence (ACAGTGCTT) was inserted between 15341T and 15342T.

The fusion sequence rendered the encoded aa [115]I unchanged, and followed by a stretch of 3 aa (QCF) insertion before the last 4 truncated aa ([116]RVT[119]A) (Fig. 5B). Nucleotide sequence comparison showed that the inserted 9-nt was a direct repeat of nt 1171–1179 (GQ330474) of nsp1 coding region, implying possible non-homologous RNA recombination between these two regions.

Growth kinetics were assessed for two plaque-purified viruses (ppvs) of CΔ3/121–123 generated in the experiment 1(Fig. 5B), including ppv7 (CΔ3/121–123 containing the Y61C mutation) that also was present in the repeated experiment, and ppv10 (CΔ3/121–123 containing residues 48–52 deletion) that had the maximal internal deletion (Fig. 5B). For CΔ4/120–123, the P5 virus containing the E51G mutation was analyzed. Fig. 4B depicts the growth curves of these mutant viruses, compared with the parental 7USC and APRRS. The CΔ3/121–123 ppv7 had a slightly lower titer than 7USC at each time point. However, the titers of CΔ3/121–123 ppv10 and CΔ4/120–123 were approximately 100-fold lower than that of 7USC, and their peaks appeared at 84 and 72 hpi, respectively, which was noticeably delayed (Fig. 4B). This suggested that the absence of the last four residues ([120]SPS[123]A) and the internal region ([48]KNPE[52]K) could adversely affected virus replication.

3.6. Internal deletion of N protein was tolerated

To further investigate whether the emergence of internal aa deletions was the result of the primary engineered deletion, or the internal aa residues *per se* were not required for N protein functionality, we introduced two internal deletions found in CΔ3/121–123 ppvs back into the wild-type pAPRRS, named as pNΔ39–42 and pNΔ48–52, respectively (Fig. 2C). Meanwhile, two double mutants containing the originally engineered C-terminal 3-aa deletion, together with second-site mutation Y61C and the residue 48–52 deletion were reconstructed. The resultant plasmids were desig-
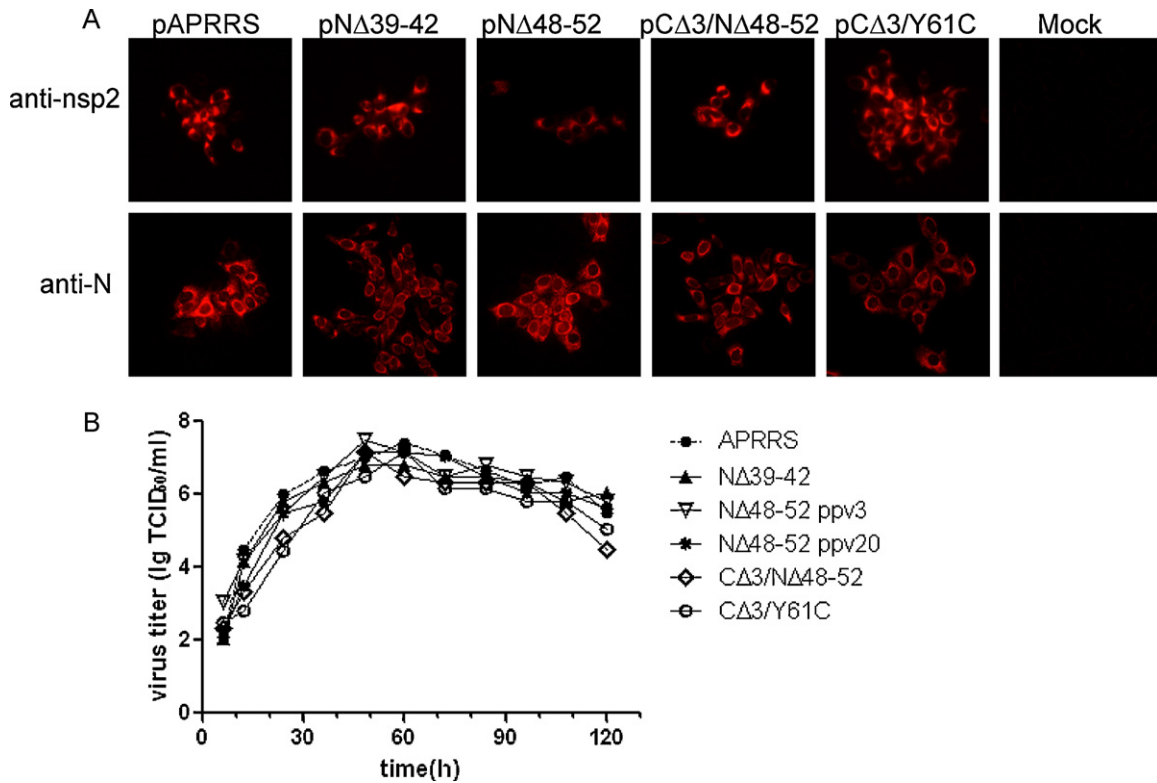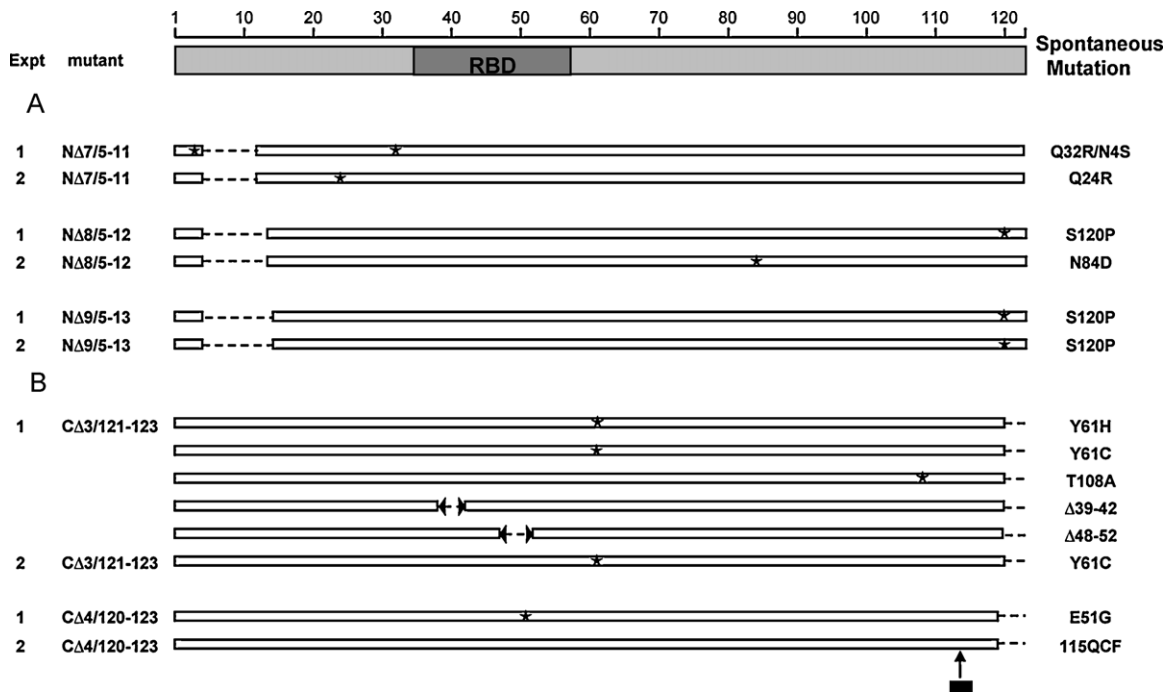
Fig. 5. Spontaneous mutations in the N protein of recovered P5 N- and C-terminal mutant viruses. Schematic representation of N protein amino acid sequence is shown at the top; RBD indicates the predicted RNA binding domain, while NLS-1 and NLS-2 represent the regions of two nuclear localization signals. The experiment (Expt) 1 and 2 indicates the independent transfection assays. The corresponding nucleotide changes are described in the text. (A) Spontaneous mutations in the N-terminal deletion mutant viruses. The positions of the engineered deletions (dashed lines) and the spontaneous substitutions (asterisks) are described relative to the schematic representation. (B) Spontaneous mutations in the C-terminal deletion mutant viruses. Dashed lines indicate the engineered deletions, whereas the asterisks represent substitutions, the broken arrows indicate sequence deletions, and the short bold line indicates the 3-aa insertion. 115QCFRVTA in experiment 2 of mutant CΔ4/120–123 indicates the fully changed final seven residues, which resulted from the 9-nt insertion between 15341T and 15342T.

Fig. 6. Infectious properties of internal deletion and double mutants. (A) Intracellular nsp2 and N expression of internal deletion mutants pNΔ39–42, pNΔ48–52, and double mutants pCΔ3/NΔ48–52 and pCΔ3/Y61C, while pAPRRS and mock transfected cells were used as controls. (B) Multiple growth curves of P5 recovered viruses on MARC-145 cells at a MOI of ~0.01.
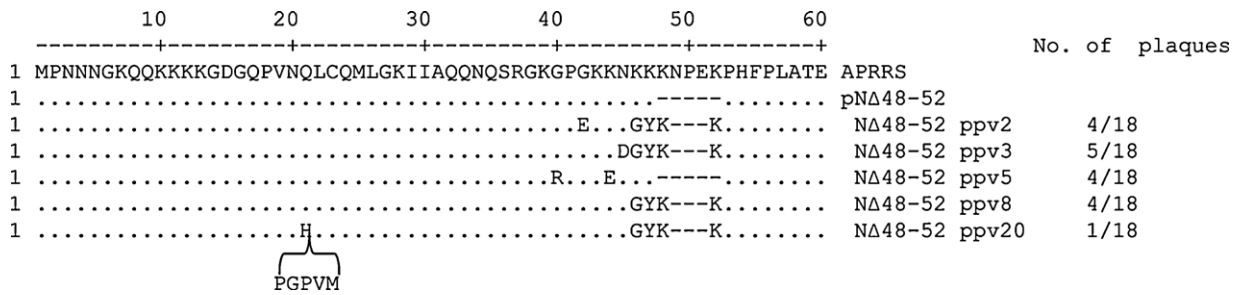
```
                10        20        30        40        50        60                      No. of  plaques
      ---------+---------+---------+---------+---------+---------+
    1 MPNNNGKQQKKKKGDGQPVNQLCQMLGKIIAQQNQSRGKGPGKKNKKKNPEKPHFPLATE  APRRS
    1 ...............................................-----........  pNΔ48-52
    1 ..............................................E...GYK---K.....  NΔ48-52 ppv2      4/18
    1 .............................................DGYK---K.........  NΔ48-52 ppv3      5/18
    1 ...............................R...E...-----........  NΔ48-52 ppv5      4/18
    1 ..............................................GYK---K.........  NΔ48-52 ppv8      4/18
    1 ....................H.........................GYK---K.........  NΔ48-52 ppv20     1/18
                          └─┘
                         PGPVM
```

Fig. 7. Multiple alignment of the first 60 aa of N protein of five different ppvs of recovered NΔ48–52, the right panel indicates the plaque numbers of each ppv. APRRS is the wild-type, whereas pNΔ48–52 indicates the engineered deletion. NΔ48–52 ppv2, ppv3, ppv5, ppv8 and ppv20 represent the different ppvs of the mutant virus NΔ48–52. The residues that match APRRS are obscured, and differed from the sequence of pNΔ48–52 are labeled. The short line indicates the deleted residues in pNΔ48–52 and recovered viruses. The 5-aa insertion in ppv20 is indicated by the brackets.

nated as pCΔ3/Y61C and pCΔ3/NΔ48–52, respectively (Fig. 2D). All of these mutant plasmids displayed nsp2 and N expression (Fig. 6A) and developed visible CPE after transfection, suggesting that the internal aa residues (^{39}KGP^{42}G) and (^{48}KNPE^{52}K) were not essential for virus viability, regardless of the presence or absence of the primary deletion.

In view of the frequent occurrence of the second-site mutations, the genetic stability of these reconstructed mutants was also investigated, but no further additional mutation was identified for recovered viruses NΔ39–42 and CΔ3/Y61C at all passage levels in the two independent transfection assays. However, mutant virus CΔ3/NΔ48–52 had yet one additional point mutation, nt A15085G (aa I30V), which was genetically stable for at least five passages. Intriguingly, no additional mutation appeared within N in the independent transfection experiment 2 in all five passages. In the case of NΔ48–52, sequence analysis indicated that the recovered viruses consisted of a mixed population in both independent experiments; viral plaque purification was therefore performed for NΔ48–52 viruses in experiment 1. Eighteen plaques were selected and sequence analysis showed five different second-site mutations, including G40R&K44E (ppv5 in Fig. 7), and four different substitutions together with 48/52K/K repaired, as summarized in Fig. 7. We further determined the master sequence of the full-length genome sequence of ppv3, no detectable genetic alteration was found in the other region of the viral genome besides N gene. It is also worth noting that the five aa (PGPVM) insertion between residues 21 and 22 of the N protein in virus NΔ48–52 ppv20 resulted in an unusual length of N protein (125 aa). Sequence comparison showed that the inserted 15-nt (CCCGGGCCCTGTCAT) was identical to a region in ORF1 (nt 12141–12155, GQ330474), which coded for nsp12 (Ziebuhr et al., 2000). Whether genomic recombination between these two regions or some other factors plays a role in this process is under investigation.

Two of the P5 ppvs of NΔ48–52 (ppv3 and ppv20 in Fig. 7), together with recovered viruses NΔ39–42, CΔ3/Y61C and CΔ3/NΔ48–52 containing the I30V substitution, were used to assess their growth properties. These viruses exhibited indistinguishable growth kinetics from the wild type APRRS (Fig. 6B), which suggested that the introduced or induced internal deletions did not affect virus replication significantly. The N protein could tolerate the internal deletion per se, which might not be related to the C-terminal engineered deletion.

4. Discussion

N protein is the most abundant and important structural protein in PRRSV virion, and plays a crucial role in virion assembly. In this study, we found that the N-terminal residues 5–13 and last four C-terminal residues were non-essential for type 2 PRRSV viability. In addition, we also demonstrated that deletion in the middle region of N protein did not block the production of infec-

tious virus. Our study is believed to be the first report that the inter-genotypically variable N terminal and internal residues of N protein could tolerate deletion without affecting type 2 PRRSV viability in cultured cells, while discrete inter-genotypically conserved terminal residues play crucial roles in viral RNA synthesis and/or virus growth. The nonessential regions identified here could be further utilized as insertion site for foreign gene tag and the rescued viruses could be the candidates for genetic marker vaccine.

The N protein of coronavirus has been shown to participating virus RNA synthesis through interacting with the transcription regulatory sequence (Grossoehme et al., 2009) or as the RNA chaperone (Zuniga et al., 2007, 2010). For arterivirus, it was documented that all of the structural proteins are not required for genomic RNA replication and sgmRNA transcription of EAV (Molenkamp et al., 2000). In this study, we demonstrated that both terminal and internal domains contained aa residues that are nonessential for virus viability. However, the replication and transcription level of some mutants were reduced, indicating PRRSV N protein and/or its coding sequence may affect viral RNA synthesis. In comparison with the PRRSV N amino acid sequence (Fig. 1A), we found that the inter-genotypically conserved residue G14 was the only difference between viable pNΔ9/5–13 and non-viable pNΔ10/5–14. It was possibly that the G14 sequence specificity was required for virus viability, which needs further site-directed mutagenesis.

We also proved that the internal residues (^{39}KGP^{42}G) and (^{48}KNPE^{52}K), respectively, were not essential for virus viability. Interestingly, these regions sandwiched the reported NLS (^{41}PGKK (N/S) K^{47}K) of N protein (Rowland et al., 1999, 2003). Lee et al. (2006) demonstrated the NLS-null mutant clone produced infectious virus, and the rescued virus displayed a titer 100-fold lower than that of wild-type virus. The mutagenized NLS underwent strong selection pressure in pig that resulted in partial or complete reversion and reacquisition of NLS function (Pei et al., 2008). In our study, the rescued virus NΔ48–52 also displayed additional mutation when transfected into the MARC-145 cells. Whether the rescued virus NΔ48–52 undergoes selective pressure in cells still needs further study.

The maximal deletion mutant virus NΔ9/5–13 and CΔ4/120–123 had severe defect on virus growth kinetics, as shown in Figs. 3D and 4B, suggesting these deletions might adversely affect virus growth. It was also worth noting that the clone pCΔ3/NΔ48–52 had identical sequence of N protein with ppv10 of CΔ3/121–123. However, the growth kinetics of ppv10 was much lower than that of CΔ3/NΔ48–52 (Figs. 4B and 6B); the only difference was that the latter had one more additional mutation I30V in N protein. Further investigation on whether the I30V substitution determines the different growth property is under way.

There are at least two experimentally identified RNA signals involving in RNA synthesis at the 3′-terminus of Arterivirus. One is the pseudoknot interaction between two 3′-proximal stem loops

(SL4 and SL5) demonstrated in EAV system (Beerens and Snijder, 2006, 2007). However, the nucleotides involved in the pseudoknot interaction in PRRSV are located in 3′UTR. Another is the kissing loop structure identified in LV strain, Verheije et al. (2002) reported that a stretch of 34 nt within LV ORF7 is essential for RNA replication because of a kissing interaction between the 7-nt sequence in ORF7 and its complementary counterpart in 3′UTR. In this study, the mutant pNΔ16/5–20 deleted part of this corresponding structure, including the putative 7-nt kissing-loop sequence in APRRS ORF7 (Fig. 1B). Therefore, we deduced that such a kissing-loop interaction might also play a role in type 2 PRRSV replication, which was supported by the failure of fluorescent signal and sgmRNA7 detection in transfected cells (Fig. 3A, C).

As a multi-functional protein, viral N protein is known for interacting with other structural protein for virion assembly (Kuo and Masters, 2002), and with RNA for genome encapsidation (Doan and Dokland, 2003). Therefore, it is necessary to investigate whether genetic alterations exist in other genomic regions. We determined the nucleotide sequences of 5′UTR, 3′UTR and M region of all mutant viruses, however, no obvious genetic alterations were observed in these regions. Therefore, the N protein domains that may be responsible for protein–RNA and protein–protein interactions are most likely located outside of the mutated region. Intriguingly, we found that a stretch of 9 nt sequence (ACAGTGCTT, nt 1171–1179) insertion in N coding region of mutant virus CΔ4/120–123 was a direct repeat from nsp1 coding region. Meanwhile, another 15-nt (CCCGGGCCCTGTCAT, nt 12141–12155) found in virus NΔ48–52 ppv20 was part of the nsp12 coding sequences. As the 9 nt insertion was out-of-frame, we speculate that such recombination most likely happened at the RNA level via non-homologous RNA recombination.

We demonstrated that the N protein truncated viruses were accompanied by multiple patterns of spontaneous mutations, whereas few missense mutations were found in other genomic regions of the P5 mutant viruses NΔ9/5–13, CΔ4/120–123, NΔ48–52 ppv3, and wild-type APRRS. We cannot completely rule out the possibility that quasispecies nature may account for some of the additional mutations, as we essentially determined the consensus sequences of the mutant viruses by direct sequencing of the RT-PCR products. Another reason for the lack of mutation is that the parental virus, APRRS, is highly adapted on MARC-145 cells, which could limit the number of the quasispecies. More importantly, these spontaneous mutations are often in the forms of deletions and insertions, which could not be simply attributed to the quasispecies nature. Our results suggested that the spontaneous mutations in N protein were caused by the introduced deletion rather than replication error.

N protein is one of the genetically conserved structural proteins. On the contrary, we found various patterns of spontaneous mutations generated from the initial terminal deletion of N protein. In present study, we did repeat transfection to investigate the properties of the spontaneous mutations. However, almost all of the recovered viruses had different additional mutations in the independent transfection assay. For example, point mutation and out-of-frame insertion were found in the recovered virus CΔ4/120–123 in two experiments (Fig. 5B). Also the same spontaneous mutation might respond to different primary deletions, such as S120P that arose simultaneously in the recovered viruses NΔ8/5–12 and NΔ9/5–13. On the other hand, most of the spontaneous mutations were located at the N-terminal domain of N protein, the structure of which is still unresolved. Therefore, it was difficult to illustrate any spatial relationship between the primary deletion and spontaneous mutations described in our study. In addition, we did not find a clear pattern of local charge compensation for the spontaneous mutations. Another explanation of the spontaneous mutations would be the role of the underlying RNA secondary structure. We also analyzed the local secondary structure of all mutants, but no significantly change was found. Except for pNΔ16/5–20, none of the other mutants and the recovered viruses affects the potential kissing loop structure of N protein. Therefore, the inherent mechanism still needs further manipulation of N protein and structural analysis of the N-terminal domain of N protein.

Taken together, we dissected the PRRSV structure–function relationship and found that (1) a stretch of inter-genotypic variable N terminal residues aa 5–13 (^{5}NGKQQKKK^{13}K) were nonessential for virus viability; (2) the last four inter-genotypic variable aa residues (^{120}SPS^{123}A) at the C terminus of N protein were dispensable for type 2 PRRSV viability; (3) the internal aa residues ranging from inter-genotypic variable aa 39–42 (^{39}KGP^{42}G) and inter-genotypic conserved 48–52 (^{48}KNPE^{52}K), respectively, were dispensable for type 2 PRRSV viability. Our results indicated the non-essential regions in N protein for PRRSV replication in cell culture, which lays a foundation for foreign gene expression and development of genetic tagged vaccine.

References

Bautista, E.M., Meulenberg, J.J., Choi, C.S., Molitor, T.W., 1996. Structural polypeptides of the American (VR-2332) strain of porcine reproductive and respiratory syndrome virus. Arch. Virol. 141 (7), 1357–1365.

Beerens, N., Snijder, E.J., 2006. RNA signals in the 3′ terminus of the genome of Equine arteritis virus are required for viral RNA synthesis. J. Gen. Virol. 87 (7), 1977–1983.

Beerens, N., Snijder, E.J., 2007. An RNA pseudoknot in the 3′ end of the arterivirus genome has a critical role in regulating viral RNA synthesis. J. Virol. 81 (17), 9426–9436.

Benfield, D.A., Nelson, E., Collins, J.E., Harris, L., Goyal, S.M., Robison, D., Christianson, W.T., Morrison, R.B., Gorcyca, D., Chladek, D., 1992. Characterization of swine infertility and respiratory syndrome (SIRS) virus (isolate ATCC VR-2332). J. Vet. Diagn. Invest. 4 (2), 127–133.

Chen, Z., Kuo, L., Rowland, R.R., Even, C., Faaberg, K.S., Plagemann, P.G., 1993. Sequences of 3′ end of genome and of 5′ end of open reading frame 1a of lactate dehydrogenase-elevating virus and common junction motifs between 5′ leader and bodies of seven subgenomic mRNAs. J. Gen. Virol. 74 (4), 643–659.

Daginakatte, G.C., Kapil, S., 2001. Mapping of the RNA-binding domain of the porcine reproductive and respiratory syndrome virus nucleocapsid protein. Adv. Exp. Med. Biol. 494, 547–552.

de Lima, M., Ansari, I.H., Das, P.B., Ku, B.J., Martinez-Lobo, F.J., Pattnaik, A.K., Osorio, F.A., 2009. GP3 is a structural component of the PRRSV type II (US) virion. Virology 390 (1), 31–36.

de Vries, A.A., Chirnside, E.D., Bredenbeek, P.J., Gravestein, L.A., Horzinek, M.C., Spaan, W.J., 1990. All subgenomic mRNAs of equine arteritis virus contain a common leader sequence. Nucleic Acids Res. 18 (11), 3241–3247.

Dea, S., Gagnon, C.A., Mardassi, H., Pirzadeh, B., Rogan, D., 2000. Current knowledge on the structural proteins of porcine reproductive and respiratory syndrome (PRRS) virus: comparison of the North American and European isolates. Arch. Virol. 145 (4), 659–688.

den Boon, J.A., Snijder, E.J., Chirnside, E.D., de Vries, A.A., Horzinek, M.C., Spaan, W.J., 1991. Equine arteritis virus is not a togavirus but belongs to the coronaviruslike superfamily. J. Virol. 65 (6), 2910–2920.

den Boon, J.A., Kleijnen, M.F., Spaan, W.J., Snijder, E.J., 1996. Equine arteritis virus subgenomic mRNA synthesis: analysis of leader-body junctions and replicative-form RNAs. J. Virol. 70 (7), 4291–4298.

Deshpande, A., Wang, S., Walsh, M.A., Dokland, T., 2007. Structure of the equine arteritis virus nucleocapsid protein reveals a dimer–dimer arrangement. Acta Crystallogr. D: Biol. Crystallogr. 63 (5), 581–586.

Doan, D.N., Dokland, T., 2003. Structure of the nucleocapsid protein of porcine reproductive and respiratory syndrome virus. Structure 11 (11), 1445–1451.

Gorbalenya, A.E., Enjuanes, L., Ziebuhr, J., Snijder, E.J., 2006. Nidovirales: evolving the largest RNA virus genome. Virus Res. 117 (1), 17–37.

Grossoehme, N.E., Li, L., Keane, S.C., Liu, P., Dann III, C.E., Leibowitz, J.L., Giedroc, D.P., 2009. Coronavirus N protein N-terminal domain (NTD) specifically binds the transcriptional regulatory sequence (TRS) and melts TRS-cTRS RNA duplexes. J. Mol. Biol. 394 (3), 544–557.

Kuo, L., Masters, P.S., 2002. Genetic evidence for a structural interaction between the carboxy termini of the membrane and nucleocapsid proteins of mouse hepatitis virus. J. Virol. 76 (10), 4987–4999.

Lee, C., Hodgins, D., Calvert, J.G., Welch, S.K., Jolie, R., Yoo, D., 2006. Mutations within the nuclear localization signal of the porcine reproductive and respiratory syndrome virus nucleocapsid protein attenuate virus replication. Virology 346, 238–250.

Meng, X.J., Paul, P.S., Morozov, I., Halbur, P.G., 1996. A nested set of six or seven subgenomic mRNAs is formed in cells infected with different isolates of porcine reproductive and respiratory syndrome virus. J. Gen. Virol. 77 (6), 1265–1270.

Meulenberg, J.J., Petersen-den Besten, A., 1996. Identification and characterization of a sixth structural protein of Lelystad virus: the glycoprotein GP2 encoded by ORF2 is incorporated in virus particles. Virology 225 (1), 44–51.

Meulenberg, J.J., de Meijer, E.J., Moormann, R.J., 1993. Subgenomic RNAs of Lelystad virus contain a conserved leader-body junction sequence. J. Gen. Virol. 74 (8), 1697–1701.

Molenkamp, R., van Tol, H., Rozier, B.C., van der Meer, Y., Spaan, W.J., Snijder, E.J., 2000. The arterivirus replicase is the only viral protein required for genome replication and subgenomic mRNA transcription. J. Gen. Virol. 81 (10), 2491–2496.

Nelsen, C.J., Murtaugh, M.P., Faaberg, K.S., 1999. Porcine reproductive and respiratory syndrome virus comparison: divergent evolution on two continents. J. Virol. 73 (1), 270–280.

Pei, Y., Hodgins, D.C., Lee, C., Calvert, J.G., Welch, S.K., Jolie, R., Keith, M., Yoo, D., 2008. Functional mapping of the porcine reproductive and respiratory syndrome virus capsid protein nuclear localization signal and its pathogenic association. Virus Res. 135, 107–114.

Rowland, R.R., Kervin, R., Kuckleburg, C., Sperlich, A., Benfield, D.A., 1999. The localization of porcine reproductive and respiratory syndrome virus nucleocapsid protein to the nucleolus of infected cells and identification of a potential nucleolar localization signal sequence. Virus Res. 64, 1–12.

Rowland, R.R., Schneider, P., Fang, Y., Wootton, S., Yoo, D., Benfield, D.A., 2003. Peptide domains involved in the localization of the porcine reproductive and respiratory syndrome virus nucleocapsid protein to the nucleolus. Virology 316, 135–145.

Snijder, E.J., Meulenberg, J.J., 1998. The molecular biology of arteriviruses. J. Gen. Virol. 79 (5), 961–979.

Spilman, M.S., Welbon, C., Nelson, E., Dokland, T., 2009. Cryo-electron tomography of porcine reproductive and respiratory syndrome virus: organization of the nucleocapsid. J. Gen. Virol. 90 (3), 527–535.

Stadejek, T., Oleksiewicz, M.B., Scherbakov, A.V., Timina, A.M., Krabbe, J.S., Chabros, K., Potapchuk, D., 2008. Definition of subtypes in the European genotype of porcine reproductive and respiratory syndrome virus: nucleocapsid characteristics and geographical distribution in Europe. Arch. Virol. 153 (8), 1479–1488.

van Nieuwstadt, A.P., Meulenberg, J.J., van Essen-Zanbergen, A., Petersen-den Besten, A., Bende, R.J., Moormann, R.J., Wensvoort, G., 1996. Proteins encoded by open reading frames 3 and 4 of the genome of Lelystad virus (Arteriviridae) are structural proteins of the virion. J. Virol. 70 (7), 4767–4772.

Verheije, M.H., Kroese, M.V., Rottier, P.J., Meulenberg, J.J., 2001. Viable porcine arteriviruses with deletions proximal to the 3′ end of the genome. J. Gen. Virol. 82 (11), 2607–2614.

Verheije, M.H., Olsthoorn, R.C., Kroese, M.V., Rottier, P.J., Meulenberg, J.J., 2002. Kissing interaction between 3′ noncoding and coding sequences is essential for porcine arterivirus RNA replication. J. Virol. 76 (3), 1521–1526.

Wensvoort, G., de Kluyver, E.P., Pol, J.M., Wagenaar, F., Moormann, R.J., Hulst, M.M., Bloemraad, R., den Besten, A., Zetstra, T., Terpstra, C., 1992. Lelystad virus, the cause of porcine epidemic abortion and respiratory syndrome: a review of mystery swine disease research at Lelystad. Vet. Microbiol. 33 (1–4), 185–193.

Wootton, S.K., Yoo, D., 2003. Homo-oligomerization of the porcine reproductive and respiratory syndrome virus nucleocapsid protein and the role of disulfide linkages. J. Virol. 77 (8), 4546–4557.

Wootton, S.K., Nelson, E.A., Yoo, D., 1998. Antigenic structure of the nucleocapsid protein of porcine reproductive and respiratory syndrome virus. Clin. Diagn. Lab. Immunol. 5 (6), 773–779.

Wootton, S., Koljesar, G., Yang, L., Yoon, K.J., Yoo, D., 2001. Antigenic importance of the carboxy-terminal beta-strand of the porcine reproductive and respiratory syndrome virus nucleocapsid protein. Clin. Diagn. Lab. Immunol. 8 (3), 598–603.

Wu, W.H., Fang, Y., Rowland, R.R., Lawson, S.R., Christopher-Hennings, J., Yoon, K.J., Nelson, E.A., 2005. The 2b protein as a minor structural component of PRRSV. Virus Res. 114 (1–2), 177–181.

Yoo, D., Wootton, S.K., Li, G., Song, C., Rowland, R.R., 2003. Colocalization and interaction of the porcine arterivirus nucleocapsid protein with the small nucleolar RNA-associated protein fibrillarin. J. Virol. 77 (22), 12173–12183.

Yu, I.M., Oldham, M.L., Zhang, J., Chen, J., 2006. Crystal structure of the severe acute respiratory syndrome (SARS) coronavirus nucleocapsid protein dimerization domain reveals evolutionary linkage between corona- and arteriviridae. J. Biol. Chem. 281 (25), 17134–17139.

Yu, D., Lv, J., Sun, Z., Zheng, H., Lu, J., Yuan, S., 2009. Reverse genetic manipulation of the overlapping coding regions for structural proteins of the type II porcine reproductive and respiratory syndrome virus. Virology 383 (1), 22–31.

Yuan, S., Wei, Z., 2008. Construction of infectious cDNA clones of PRRSV: separation of coding regions for nonstructural and structural proteins. Sci. China C: Life Sci. 51 (3), 271–279.

Zheng, H., Sun, Z., Zhu, X.Q., Long, J., Lu, J., Lv, J., Yuan, S., 2010. Recombinant PRRSV expressing porcine circovirus sequence reveals novel aspect of transcriptional control of porcine arterivirus. Virus Res. 148 (1–2), 8–16.

Ziebuhr, J., Snijder, E.J., Gorbalenya, A.E., 2000. Virus-encoded proteinases and proteolytic processing in the Nidovirales. J. Gen. Virol. 81 (4), 853–879.

Zuniga, S., Sola, I., Moreno, J.L., Sabella, P., Plana-Duran, J., Enjuanes, L., 2007. Coronavirus nucleocapsid protein is an RNA chaperone. Virology 357 (2), 215–227.

Zuniga, S., Cruz, J.L., Sola, I., Mateos-Gomez, P.A., Palacio, L., Enjuanes, L., 2010. Coronavirus nucleocapsid protein facilitates template switching and is required for efficient transcription. J. Virol. 84 (4), 2169–2175.